J Supercond Nov Magn (2014) 27:9–15
DOI 10.1007/s10948-013-2405-z

REVIEW PAPER

An Overview on the Research of Iron-Based High-T_c Superconductors Probed by X-ray Absorption Spectroscopy

Jie Cheng · Wangsheng Chu · Shengli Liu · Peng Dong · Ziyu Wu

Received: 21 September 2013 / Accepted: 15 October 2013 / Published online: 10 November 2013
© Springer Science+Business Media New York 2013

Abstract The discovery in 2008 of a new family of high-T_c superconductor (HTSC), i.e., layered compounds based on iron, has spurred a tremendous interest in the community of condensed matter physics. This discovery has broken cuprate "monopoly" in the physics of HTSC materials. Until now, thousands of experimental and theoretical methods were devoted to investigate the superconducting properties of this new iron-based HTSCs. Synchrotron radiation-based X-ray absorption spectroscopy (XAS) made great contributions to the local lattice structure, the electronic structure, and even the superconductive mechanism of this iron-based materials. The aim of this review is a short introduction into the progress of research on new iron-based HTSCs probed by the unique technique—XAS, including the electron correlations, local lattice distortions, changes of valence upon doping or pressure, and even the isotope effect for this new iron-based family.

J. Cheng (✉)
College of Science, Nanjing University of Posts and Telecommunications, Nanjing, Jiangsu 210023, China
e-mail: chengj@njupt.edu.cn

J. Cheng · W. Chu · Z. Wu
National Synchrotron Radiation Laboratory, University of Science and Technology of China, Hefei, Anhui 230029, China

W. Chu · Z. Wu
Beijing Synchrotron Radiation Facility, Institute of High Energy Physics, Chinese Academy of Sciences, Beijing 100049, China

S. Liu
Nanjing University (Suzhou) High-tech Institute, Nanjing, Jiangsu 215123, China

P. Dong
College of Tongda, Nanjing University of Posts and Telecommunications, Nanjing, Jiangsu 210023, China

Keywords Iron-based superconductors · XAS · Local structure · Electronic structure · Isotope effect

1 Introduction

Superconductivity is one of the most widely studied quantum phenomena in solid-state physics. Even a minor increase in the superconducting temperature (T_c) can greatly ease the practical handling and application of superconductors. Previously, high-T_c has only been observed in cuprates [1]; in February 2008, the discovery of 26 K superconductivity in fluorine-doped LaFeAsO with the primitive tetragonal ZrCuSiAs-type (1111-type) structure [2], has attracted a tremendous interest, marking the beginning of worldwide efforts to investigate this new family of superconductors [3, 4]. Subsequently, by replacing the La atoms with other rare-earth elements and modulating the structural parameters, T_c was quickly enhanced in $SmFeAsO_{1-x}F_x$, $CeFeAsO_{1-x}F_x$, $PrFeAsO_{1-x}F_x$, and $NdFeAsO_{1-x}F_x$ to above 50 K [5–8]. And then the superconductivity in K-doped $BaFe_2As_2$ (122-type), Li_xFeAs (111-type) and $FeSe_{1-x}$ were reported successively [9–11].

The first and probably most urgent question to answer regards the superconductive mechanism of iron-based high-T_c superconductors (HTSCs). Is it the same as copper-based materials due to the many similarities? Actually, both cuprates and iron-based ones are layered systems and the crystal structure of iron-based compounds contains the FeAs superconductive layer with Fe atoms in a square planar lattice arrangement, like the characteristic CuO_2 layer in cuprates. Moreover, the phase diagram of both systems exhibits the competition between antiferromagnetism and superconductivity [12, 13]. But more and more observations of the isotope effect in iron-based superconductors

pointed out that superconductivity in these new materials may be much different from cuprate superconductors. Due to above considerations, almost all researches have been focused on the structural, electronic, and magnetic behaviors revealing many important physical properties. Thereinto, Synchrotron radiation-based X-ray absorption spectroscopy (XAS) played an important role in investigating the electronic structure, local lattice structure, and even the superconductive mechanism of this new family of superconductors. Here, this review article mainly provides a short introduction of the research of iron-based materials probed by the unique technique—XAS.

2 Information from XAS

As we know, material properties are in a close relationship with its atomic structure and electronic structure. For these newly discovered iron-based superconductors, doping elements can finely modulate the lattice structure, and then the electronic/magnetic structure and superconductive properties of the system can be modified. As a consequence, investigations of the local lattice structure as well as the electronic structure are greatly important for clarifying the superconductive mechanism of iron-based superconductors.

X-ray diffraction (XRD) is a conventional method to study the structure; it can only return the average long-range-order parameter, not sensitive to the local structural distortions induced by dopants, while XAS is a powerful element-selective local structural probe and has been effective in investigating both the local lattice and electronic structure of a material. Furthermore, synchrotron radiation offers X-rays of very high intensity with a broad spectral distribution, ideally suited for XAS. Therefore, synchrotron radiation-based XAS is no doubt a better technical method to study the relationship between the local lattice structure and the superconductive mechanism of iron-based materials.

The absorption of X-rays by matter as a function of their energy is characterized by a smoothly varying background absorption and by characteristic jumps of the absorption coefficient, which are called absorption edges E_0. XAS refers to the oscillatory structure in the absorption coefficient just above the absorption edge, and can be divided into two components, which differ in their physical origin (in Fig. 1). The X-ray absorption near-edge structure (XANES) comprises the regime from -10 eV below to about $+50$ eV above E_0, characterized by rather sharp variations of the absorption. In the part from $+50$ eV to $+1000$ eV above E_0, weak oscillations occur. These are designated as extended X-ray absorption fine structure (EXAFS).

Features of the XANES in the preedge region are related to electronic transitions from core levels into unoccupied electronic states located at the absorbing atom. Therefore,

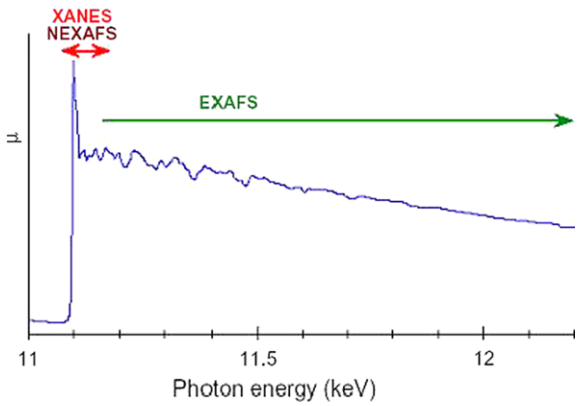

Fig. 1 XAS is divided into XANES and EXAFS

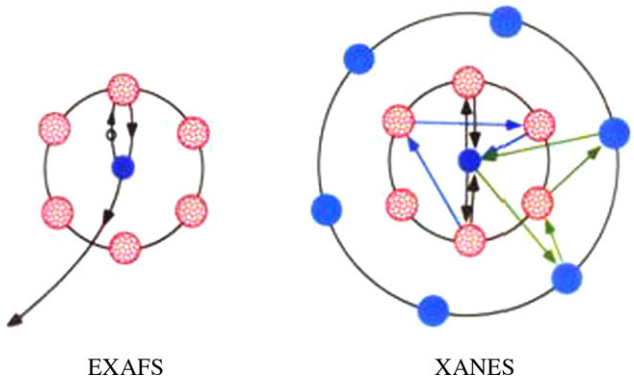

Fig. 2 The single and multiple scattering of the electron between the absorbed atom and the surrounding atoms

the shape of the preedge features and their intensity can give us some detailed information about the electronic and also the geometric structure, for example, the distortion of coordination environments. Moreover, features of the XANES above E_0 and those in the EXAFS regime can be traced back to the scattering of the electron between the absorbing atom and the surrounding atoms (in Fig. 2). In the XANES, multiple scattering of the electron can occur, and the theoretical description of this region is thus rather complex. However, most of the features of the EXAFS region can be explained quantitatively by singly scattering of the excited electron. Thus, EXAFS contains the information of interatomic distances R, coordination numbers N and the temperature-dependent fluctuation in bond length σ^2, which should also include effects due to structural disorder. As a consequence, we can get manifold information about the geometrical (EXAFS and XANES) and electronic (XANES) structure of the system.

3 Research of Iron-Based Superconductors by XAS

During these years, almost all the techniques were devoted to different aspects of superconductivity in this new family

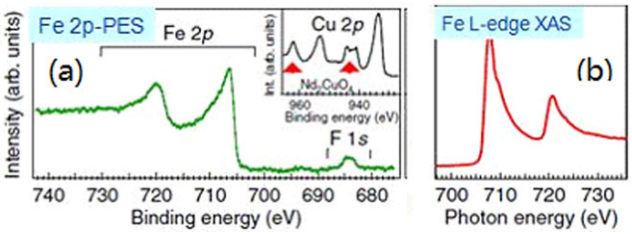

Fig. 3 (**a**) The PES spectrum of iron-based $CeFeAsO_{0.89}F_{0.11}$ and cuprate Nd_2CuO_4. (**b**) Fe L_{23}-edge XAS of $CeFeAsO_{0.89}F_{0.11}$

of iron-based HTSCs. To further understand the superconductive properties and even their superconductive mechanism, synchrotron radiation-based XAS techniques were applied and made great contributions in the following aspects.

3.1 Electron Correlations

A hallmark of cuprate HTSCs which sets them apart from conventional BCS-like superconductors is their anomalies of the normal state (inapplicability of Fermi-liquid theory), which are related to the strong electron correlations. That is why the physical nature of high-T_c superconductivity in cuprates is still not completely understood. Thus, a description of the electron correlations in iron-based HTSCs is expected to establish the commonalities and differences with the cuprate HTSCs, and to describe the physics of this new family of materials.

In [14], Bondino et al. studied the electron correlations of iron-based HTSCs for the first time. From Fig. 3, the Cu 2p photoemission spectroscopy (PES) in cuprate Nd_2CuO_4 is characterized by satellite structures as a result of the localized character of the Cu 3d electrons, while the Fe 2p spectrum in $CeFeAsO_{0.89}F_{0.11}$ exhibits a main $2p_{3/2}$ peak, which is markedly different from that of Fe ionic compounds but more akin to that of the Fe metal. Similar conclusions were reached from inspection of the Fe L_{23}-edge XAS. The absence of well-defined multiplet structures renders the line shape markedly different compared with those of iron ionic oxides and much more similar to that of Fe metal, a feature indicative of delocalization of the Fe 3d band states.

Actually, [14] initiated the investigation of electron correlations in iron-based HTSCs by XAS, since then many reports pointed out the itinerant character of Fe 3d electrons of 122-type and 111-type iron HTSCs. For example, Yang et al. showed that the XAS spectra for 122 and 1111-type Fe pnictides are qualitatively similar to Fe metal; furthermore, density-functional calculations obtained Hubbard parameters of $U \sim 2$ eV and $J \sim 0.8$ eV, the values of electron correlations are much smaller than that of the cuprates [15].

In summary, the iron-based HTSCs are quite unique, which are typical of itinerant electrons, without the signatures of strong local electron correlations that characterized by cuprate HTSCs.

3.2 Local Lattice Structure with Atomic Scale

It is well known, EXAFS fitting can provide the information of local lattice structure; meanwhile, by applying EAXFS in a temperature-dependent experiment, useful lattice dynamic information, such as the Einstein frequency and local force constant of atomic bond, can also be quantitatively estimated.

At first, Zhang et al. reported the temperature-dependent local lattice distortions in the Fe–As bond mean square relative displacement (MSRD) of 1111-type HTSCs (i.e., $LaFeAsO_{1-x}F_x$ and $SmFeAsO_{1-x}F_x$), indicating a strong electron-lattice interaction in oxypnictide superconductors [16, 17]. After that, in [18] the potassium doping effect on the local lattice structure of $Ba_{1-x}K_xFe_2As_2$ was studied by temperature-dependent Fe and As-edge EXAFS. In Fig. 4, the data exhibits a softer Fe–Fe bond in a K-doped sample. Moreover, in $NdFeAsO_{1-x}F_x$ compounds Joseph et al. found that the Fe–As bond length seems to get harder in the superconducting regime [19]. Then they concluded the temperature dependence of the MSRD of the Fe–As bond for the 1111-type iron-based HTSCs. Data present a clear increase in the force constant of the Fe–As bonds, with increasing rare-earth size in the 1111-type materials [19]. The above observations are an indication of the nonnegligible role of the lattice modes (especially at FeAs superconductive layers) in the superconductivity of these iron-based materials.

For 11-type $FeSe_{1-x}Te_x$ superconductor, the Fe–Se (Fe-Te) bond length was found to be much shorter (longer) than the average Fe–Se/Te, indicating distinct site occupation by the Se and Te atoms [20]. Results provide a clear evidence of local inhomogeneities with coexisting electronic components, having direct implication on the low lying electronic states and magnetic order, pointing out a possible route to understand the physics of iron-based 11-type superconductors.

Several investigations already established a correlation between the superconductive behavior of Fe-based superconductors and the topology of $FeAs_4$ tetrahedra and anion distance from the Fe layer [21–23]. Data showed that T_c increases as the $FeAs_4$ coordination approach a regular tetrahedron [21]. Moreover, for a typical Fe-based superconductor, 1.38 Å is the optimal anion height to achieve the highest T_c [23]. In [24], using the Fe–As and Fe–Fe bond lengths obtained by EXAFS analysis, Cheng et al. presented the Fe–As–Fe bond angle and the As height as a function of both F and Zn concentration in (F,Zn)-codoped LaFeAsO superconductor in Fig. 5. In the F-underdoped region, Zn doping leads to a more symmetric $FeAs_4$ coordination while T_c increases accordingly. On the contrary, the $FeAs_4$ tetrahedron is distorted by Zn doping and a severe suppression of the superconductivity in the F-overdoped regime is observed. This

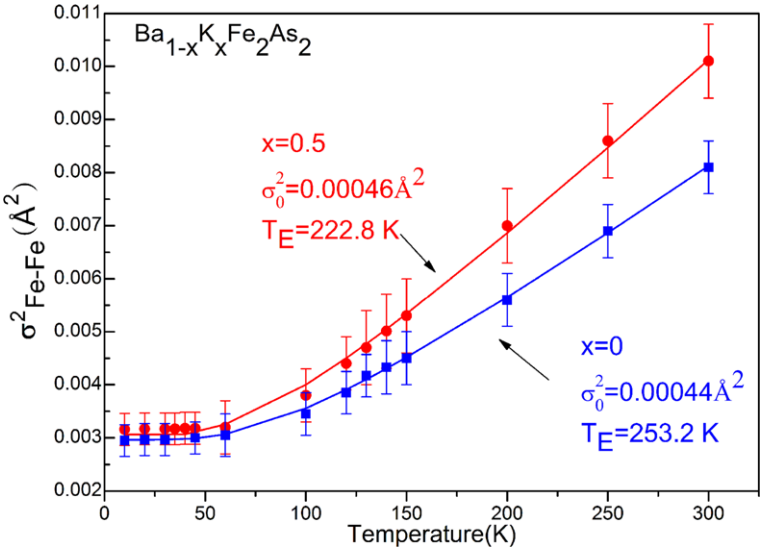

Fig. 4 Temperature-dependent σ^2 (symbols) of the Fe–Fe pair for the $Ba_{1-x}K_xFe_2As_2$ ($x = 0$ and 0.5) samples and their simulations using the classical Einstein model (*solid lines*)

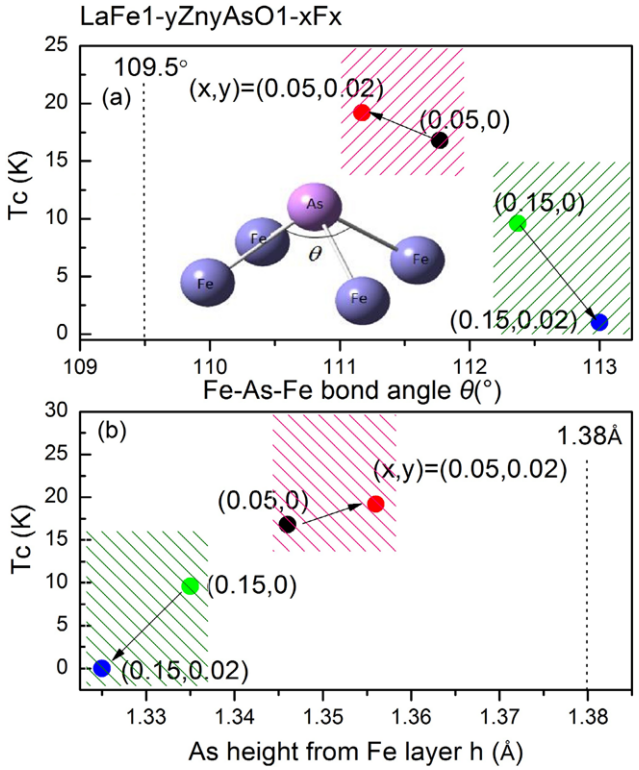

Fig. 5 The Fe–As–Fe bond angle (**a**) and the height of the As from the Fe layer (**b**) in the (F,Zn)-codoped LaFeAsO superconductor

new finding of the local structural deformation may provide an interesting insight toward understanding the interaction of multiple impurities in iron-based HTSCs.

3.3 The Changes of Valence upon Doping or Pressure

Sun et al. applied pressure-dependent Ce-L_3 XAS to investigate the electronic structure of $CeFeAsO_{1-x}F_x$ superconductors [25]. In Fig. 6, it was found that with increasing pressure the intensity of the main peak (associated with the $4f^1$ configuration) was suppressed, while the intensity of $4f^0$ satellite peak increased at the same time. Then implying a widely used method $\upsilon = 3 + I_{\text{satellite}}/(I_{\text{main}} + I_{\text{satellite}})$, they found the mean valence of Ce ions (υ) has a small change upon increasing pressure, varying from 3.0 at 1 GPa to 3.1 at 11.3 GPa. What is more, the high-pressure behavior in $CeFeAsO_{1-x}F_x$ resembles the γ–α phase transition under high pressure in Ce metal (in Fig. 6(c)), suggesting an intimate relationship between the superconductivity and Kondo effect in $CeFeAsO_{1-x}F_x$.

In Fig. 7, Sun et al. also analyzed the Eu-L_3 XAS of $EuFe_2As_2$, pointing out that either chemical pressure (e.g., P-doping) or physical pressure can induce a clear change of the Eu valence from divalent to trivalent state [26]. These valence changes make Eu layers provide additional charges to the superconductive FeAs layers, which have a positive contribution to the superconducting properties. Furthermore, Yamaoka et al. found in $CeFeAsO_{1-y}$ an upper limit of 3.0 is suggested for the Ce valence, beyond which the superconductivity is suppressed [27].

We believe that the evidence of chemical and physical pressure-induced valence changes probed by XAS could introduce a new clue for experimental studies on the synthesis of superconductors and unfold a way to investigate the physical mechanism of superconductivity in iron-based HTSCs.

3.4 Isotope Effect

In modern condensed matter physics, one of the most challenging problems is the origin of the superconductivity in HTSCs. Two decades of efforts based on thousands of experimental and theoretical researches pointed out that electron–electron interaction (EEI) rather than the electron–phonon

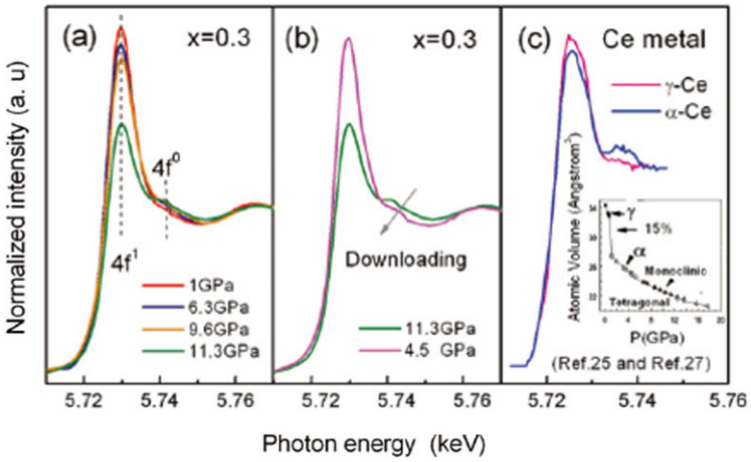

Fig. 6 Ce-L_3 XAS of $CeFeAsO_{0.7}F_{0.3}$ sample (**a**) upon unloading and (**b**) downloading, and (**c**) XAS data of the γ and α phases in Ce metal

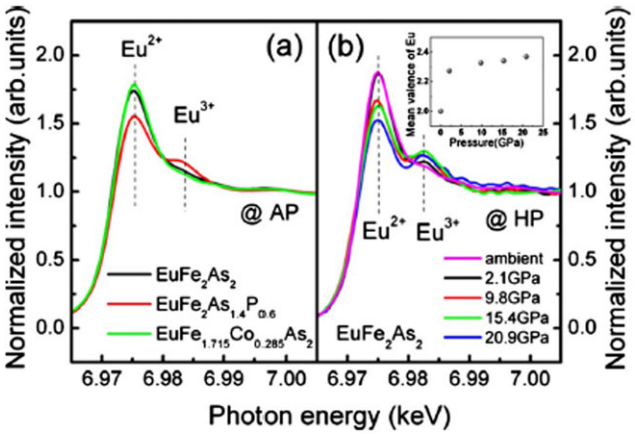

Fig. 7 Eu-L_3 XAS data obtained (**a**) at ambient pressure for three $EuFe_2As_2$-based material (**b**) at high pressure for $EuFe_2As_2$ sample

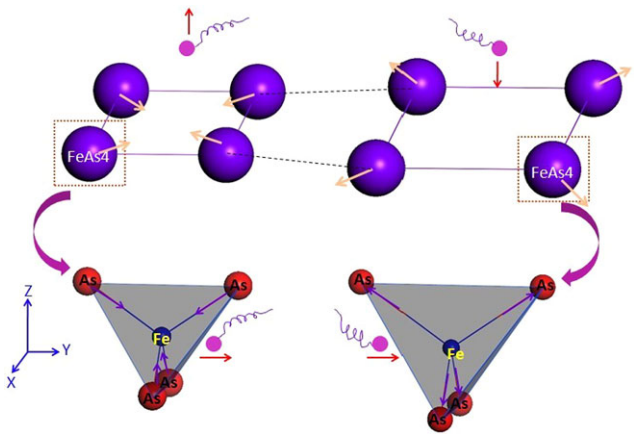

Fig. 8 Layout of Fe–Fe and Fe–As vibrations in the iron-based HTSCs. Fe–Fe bonds are in the superconducting layers and their vibrations attract electrons in the *c* direction, while Fe–As bonds are oriented along the *c* axis and their vibrations affect electrons in the *a–b* layers

interaction (EPI) plays a significant role to trigger the superconductivity in the cuprate HTSCs. However, for this new family of iron-based HTSCs, a clear iron isotope effect was experimentally observed [28–31]. Firstly, Liu et al. found a large and positive iron isotope effect (Fe-IE) on T_c in both $SmFeAsO_{1-x}F_x$ and $Ba_{1-x}K_xFe_2As_2$ superconductors, well beyond the BCS value [28]. Then Khasanov et al. observed an Fe-IE exponent of 0.8 in the $FeSe_{1-x}$ system [29]. Finally, Shirage et al. reported an inverse Fe-IE in the $Ba_{1-x}K_xFe_2As_2$ superconductor [30]. More recently, Khasanov et al. tried solving the discrepancy in the Fe-IE measurements by separating the exponent in two terms: one related to structural changes and one intrinsic [32]. And they also emphasized that the Fe isotope substitution causes small structural modifications which, in turn, may affect T_c. Therefore, additional and more accurate experimental methods to measure the Fe-IE, probing not only macroscopic averaged properties such as those based on T_c determinations, but also microscopic information of the iron-based HTSCs are required.

Chu et al. present an investigation of the Fe-IE in $Ba_{1-x}K_xFe_2As_2$ system by temperature-dependent EXAFS in the framework of Einstein model [33]. They measured both Fe and As-edge EXAFS of the $Ba_{0.6}K_{0.4}Fe_2As_2$ system by replacing ^{56}Fe (^{56}Fe-sample) with the isotope ^{54}Fe (^{54}Fe-sample). This method can separate the static structural isotope contribution and the local lattice isotope contribution. Data pointed out that the isotope substitution has a negligible effect on interatomic distances. While both the local vibrations of the Fe–As and Fe–Fe bonds show strong Fe isotope dependence (in Table 1), which is a marker of an intrinsic isotope effect.

Because Fe–Fe bonds lie in the superconductive layers (*a–b* plane) while Fe–As bonds are oriented along the *c* axis, the result pointed out the 3D-EPI in the iron-based HTSCs as shown in Fig. 8, which is much different from the layered cuprate HTSCs. In summary, the temperature-dependent EXAFS method represents the first experimental

Table 1 Values of local static distortions and Einstein temperatures associated to the Fe–As and Fe–Fe bonds in the ^{54}Fe- and ^{56}Fe-samples

Bonds	Isotope	σ_0^2 (Å^2)	T_E (K)	Fe-IE coefficient (α)
Fe–As	^{54}Fe-sample	0.0025 ± 0.0002	331.5 ± 2.0	0.37
	^{56}Fe-sample	0.0024 ± 0.0002	327.1 ± 2.0	
Fe–Fe	^{54}Fe-sample	0.0056 ± 0.0002	169.0 ± 1.0	0.41
	^{56}Fe-sample	0.0053 ± 0.0002	166.5 ± 1.0	

link between the Fe-IE and the superconducting mechanism at a microscopic level.

4 Summary and Outlook

In this review, the many important progresses on the iron-based materials by XAS have been summarized. Results show that the iron-based HTSCs are characterized by itinerant electrons, i.e., the value of electron interactions on iron-based compounds is much smaller than that of cuprate material, which is the strongly correlated system. Moreover, upon chemical pressure (i.e., doping) or physical pressure the local lattice structure and the electronic structure (e.g., the valence changes) are finely modulated. Finally, the temperature-dependent EXAFS method represents the first experimental link between the Fe-IE and the superconducting mechanism at a microscopic level, providing a clear evidence of the electron–phonon interaction in iron-based materials, much different from the cuprates characterized by the strong electron–electron interaction.

Progress in this field is rather spectacular and rapid, so that this review may be in no sense exhaustive. Moreover, they are many important questions concerning the iron-based HTSCs that remain to be answered, and whether or not the superconducting mechanism in these systems is driven by electron–phonon interaction needs further experimental and theoretical studies.

Acknowledgements This work was partly supported by the Natural Science Foundation of Jiangsu Province of China (Nos. BK20130855 and BK20130376), the National Natural Science Foundation of China (No. 11179023) and the Scientific Research Foundation of Nanjing University of Posts and Telecommunications (No. NY213053).

References

1. Bednorz, J.G., Muller, K.A.: Possible high T_c superconductivity in the Ba–La–Cu–O system. Z. Phys. B **64**, 189–193 (1986)
2. Kamihara, Y., Watanabe, T., Hirano, M., Hosono, H.: Iron-based layered superconductor La[$O_{1-x}F_x$]FeAs ($x = 0.05$–0.12) with $T_c = 26$ K. J. Am. Chem. Soc. **130**, 3296–3297 (2008)
3. Chiao, M.: Superconductivity: has lightning struck twice? Nat. Phys. **4**, 446 (2008)
4. Grant, P.M.: Superconductivity: prospecting for an iron age. Nature **453**, 1000–1001 (2008)
5. Chen, X.H., Wu, T., Wu, G., Liu, R.H., Chen, H., Fang, D.F.: Superconductivity at 43 K in $SmFeAsO_{1-x}F_x$. Nature **453**, 761–762 (2008)
6. Chen, G.F., Li, Z., Wu, D., Li, G., Hu, W.Z., Dong, J., Zheng, P., Luo, J.L., Wang, N.L.: Superconductivity at 41 K and its competition with spin-density-wave instability in layered $CeO_{1-x}F_xFeAs$. Phys. Rev. Lett. **100**, 247002 (2008)
7. Ren, Z.A., Yang, J., Lu, W., Yi, W., Che, G.C., Dong, X.L., Sun, L.L., Zhao, Z.X.: Superconductivity at 52 K in iron based F doped layered quaternary compound Pr[$O_{1-x}F_x$]FeAs. Mater. Res. Innov. **12**, 105 (2008)
8. Ren, Z.A., Yang, J., Lu, W., Yi, W., Shen, X.L., Li, Z.C., Che, G.C., Dong, X.L., Sun, L.L., Zhou, F., Zhao, Z.X.: Superconductivity in the iron-based F-doped layered quaternary compound Nd[O_{1-x}]FeAs. Europhys. Lett. **82**, 57002 (2008)
9. Rotter, M., Pangerl, M., Tegel, M., Johrendt, D.: Superconductivity and crystal structures of $(Ba_{1-x}K_x)Fe_2As_2$ ($x = 0$–1). Angew. Chem. Int. Ed. **47**, 7949–7952 (2008)
10. Wang, X.C., Liu, Q.Q., Lv, Y.X., Gao, W.B., Yang, L.X., Yu, R.C., Li, F.Y., Jin, C.Q.: The superconductivity at 18 K in LiFeAs system. Solid State Commun. **148**, 538 (2008)
11. Margadonna, S., Takabayashi, Y., McDonald, M.T., Kasperkiewicz, K., Mizuguchi, Y., Takano, Y., Fitch, A.N., Suard, E., Prassides, K.: Crystal structure of the new $FeSe_{1-x}$ superconductor. Chem. Commun. **2008**, 5607–5609 (2008)
12. Rotundu, C.R., Keane, D.T., Freelon, B., Wilson, S.D., Kim, A., Valdivia, P.N., Bourret-Courchesne, E., Birgeneau, R.J.: Phase diagram of the $PrFeAsO_{1-x}F_x$ superconductor. Phys. Rev. B **80**, 144517 (2009)
13. Chen, H., Ren, Y., Qiu, Y., Bao, W., Liu, R.H., Wu, G., Wu, T., Xie, Y.L., Wang, X.F., Huang, Q., Chen, X.H.: Coexistence of the spin-density wave and superconductivity in $Ba_{1-x}K_xFe_2As_2$. Europhys. Lett. **85**, 17006 (2009)
14. Bondino, F., Magnano, E., Malvestuto, M., Parmigiani, F., McGuire, M.A., Sefat, A.S., Sales, B.C., Jin, R., Mandrus, D., Plummer, E.W., Singh, D.J., Mannella, N.: Evidence for strong itinerant spin fluctuations in the normal state of $CeFeAsO_{0.89}F_{0.11}$ iron-oxypnictide superconductors. Phys. Rev. Lett. **101**, 267001 (2008)
15. Yang, W.L., Sorini, A.P., Chen, C.C., Moritz, B., Lee, W.S., Vernay, F., Olalde-Velasco, P., Denlinger, J.D., Delley, B., Chu, J.H., Analytis, J.G., Fisher, I.R., Ren, Z.A., Yang, J., Lu, W., Zhao, Z.X., van den Brink, J., Hussain, Z., Shen, Z.X., Devereaux, T.P.: Evidence for weak electronic correlations in iron pnictides. Phys. Rev. B **80**, 014508 (2009)
16. Zhang, C.J., Oyanagi, H., Sun, Z.H., Kamihara, Y., Hosono, H.: Low-temperature lattice structure anomaly in the $LaFeAsO_{0.93}F_{0.07}$ superconductor by x-ray absorption spectroscopy: evidence for a strong electron–phonon interaction. Phys. Rev. B **78**, 214513 (2008)
17. Zhang, C.J., Oyanagi, H., Sun, Z.H., Kamihara, Y., Hosono, H.: Electronic and lattice structures in $SmFeAsO_{1-x}F_x$ probed by x-ray absorption spectroscopy. Phys. Rev. B **81**, 094516 (2010)
18. Cheng, J., Chu, W.S., Wu, G., Zhao, H.F., Xu, W., Zhou, J., Zhang, L.J., Chen, X.H., Wu, Z.Y.: Potassium doping effect on the lattice softening and electronic structure of $Ba_{1-x}K_xFe_2As_2$ probed by

X-ray absorption spectroscopy. J. Synchrotron Radiat. **17**, 730–736 (2010)
19. Joseph, B., Iadecola, A., Malavasi, L., Saini, N.L.: Temperature-dependent local structure of $NdFeAsO_{1-x}F_x$ system using arsenic K-edge extended x-ray absorption fine structure. J. Phys. Condens. Matter **23**, 265701 (2011)
20. Joseph, B., Iadecola, A., Puri, A., Simonelli, L., Mizuguchi, Y., Takano, Y., Saini, N.L.: Evidence of local structural inhomogeneity in $FeSe_{1-x}Te_x$ from extended x-ray absorption fine structure. Phys. Rev. B **82**, 020502 (2010)
21. Lee, C.H., Iyo, A., Eisaki, H., Kito, H., Fernandez-Diaz, M.T., Ito, T., Kihou, K., Matsuhata, H., Braden, M., Yamada, K.: Effect of structural parameters on superconductivity in fluorine-free $LnFeAsO_{1-y}$ (Ln = La, Nd). J. Phys. Soc. Jpn. **77**, 083704 (2008)
22. Kuroki, K., Usui, H., Onari, S., Arita, R., Aoki, H.: Pnictogen height as a possible switch between high-T_c nodeless and low-T_c nodal pairings in the iron-based superconductors. Phys. Rev. B **79**, 224511 (2009)
23. Mizuguchi, Y., Hara, Y., Deguchi, K., Tsuda, S., Yamaguchi, T., Takeda, K., Tou, H., Takano, Y.: Anion height dependence of T_c for the Fe-based superconductor. Supercond. Sci. Technol. **23**, 054013 (2010)
24. Cheng, J., Zhou, J., Hu, R., Xu, W., Li, Y.K., Zhang, L.J., Marcelli, A., Chu, W.S., Xu, Z.A., Wu, Z.Y.: Charge redistribution and local lattice structure of (F,Zn)-codoped LaFeAsO superconductor. New J. Phys. **14**, 033005 (2012)
25. Sun, L.L., Dai, X., Zhang, C., Yi, W., Chen, G.F., Wang, N.L., Zheng, L.R., Jiang, Z., Wei, X.J., Huang, Y.Y., Yang, J., Ren, Z.A., Lu, W., Dong, X.L., Che, G.C., Wu, Q., Ding, H., Liu, J., Hu, T.D., Zhao, Z.X.: Pressure-induced competition between superconductivity and Kondo effect in $CeFeAsO_{1-x}F_x$ ($x = 0.16$ and 0.3). Europhys. Lett. **91**, 57008 (2009)
26. Sun, L., Guo, J., Chen, G., Chen, X., Dong, X., Lu, W., Zhang, C., Jiang, Z., Zou, Y., Zhang, S., Huang, Y., Wu, Q., Dai, X., Li, Y., Liu, J., Zhao, Z.: Valence change of europium in $EuFe_2As_{1.4}P_{0.6}$ and compressed $EuFe_2As_2$ and its relation to superconductivity. Phys. Rev. B **82**, 134509 (2010)
27. Yamaoka, H., Jarrige, I., Ikeda-Ohno, A., Tsutsui, S., Lin, J.-F., Takeshita, N., Miyazawa, K., Iyo, A., Kito, H., Eisaki, H., Hiraoka, N., Ishii, H., Tsuei, K.D.: Hybridization and suppression of superconductivity in $CeFeAsO_{1-y}$: pressure and temperature dependence of the electronic structure. Phys. Rev. B **82**, 125123 (2010)
28. Liu, R.H., Wu, T., Wu, G., Chen, H., Wang, X.F., Xie, Y.L., Ying, J.J., Yan, Y.J., Li, Q.J., Shi, B.C., Chu, W.S., Wu, Z.Y., Chen, X.H.: A large iron isotope effect in $SmFeAsO_{1-x}F_x$ and $Ba_{1-x}K_xFe_2As_2$. Nature **459**, 64–67 (2009)
29. Khasanov, R., Bendele, M., Conder, K., Keller, H., Pomjakushina, E., Pomjakushin, V.: Iron isotope effect on the superconducting transition temperature and the crystal structure of $FeSe_{1-x}$. New J. Phys. **12**, 073024 (2010)
30. Shirage, P.M., Kihou, K., Miyazawa, K., Lee, C.-H., Kito, H., Eisaki, H., Yanagisawa, T., Tanaka, Y., Iyo, A.: Inverse iron isotope effect on the transition temperature of the $(Ba,K)Fe_2As_2$ superconductor. Phys. Rev. Lett. **103**, 257003 (2009)
31. Shirage, P.M., Miyazawa, K., Kihou, K., Kito, H., Yoshida, Y., Tanaka, Y., Eisaki, H., Iyo, A.: Absence of an appreciable iron isotope effect on the transition temperature of the optimally doped $SmFeAsO_{1-y}$ superconductor. Phys. Rev. Lett. **105**, 037004 (2010)
32. Khasanov, R., Bendele, M., Bussmann-Holder, A., Keller, H.: Intrinsic and structural isotope effects in iron-based superconductors. Phys. Rev. B **82**, 212505 (2010)
33. Chu, W., Cheng, J., Chu, S., Hu, T., Marcelli, A., Chen, X., Wu, Z.: Iron isotope effect and local lattice dynamics in the $(Ba,K)Fe_2As_2$ superconductor studied by temperature-dependent EXAFS. Sci. Rep. **3**, 1750 (2013)